AGU PUBLICATIONS

Geophysical Research Letters

RESEARCH LETTER

10.1002/2015GL063972

Key Points:

- SIC reemergence signals highly dependent on model formulation
- SIC reemergence patterns set by SLP teleconnections in fully coupled models
- Ocean provides memory source for reemergence, and atmosphere provides variability

Supporting Information:

- Text S1, Figure S1, and Caption of Movie S1
- Movie S1

Correspondence to:
M. Bushuk,
bushuk@cims.nyu.edu

Citation:
Bushuk, M., and D. Giannakis (2015), Sea-ice reemergence in a model hierarchy, *Geophys. Res. Lett.*, *42*, 5337–5345, doi:10.1002/2015GL063972.

Received 30 MAR 2015
Accepted 27 MAY 2015
Accepted article online 29 MAY 2015
Published online 3 JUL 2015

Sea-ice reemergence in a model hierarchy

Mitchell Bushuk[1] and Dimitrios Giannakis[1]

[1]Courant Institute of Mathematical Sciences, New York University, New York, New York, USA

Abstract Lagged correlation analysis of Arctic sea-ice area reveals that melt season sea-ice anomalies tend to recur the following growth season, and growth season anomalies tend to recur the following melt season. In this work, a climate model hierarchy is used to investigate the relative role of the atmosphere and the ocean in driving this phenomenon, termed sea-ice reemergence. The covariability of sea-ice concentration (SIC), sea surface temperature (SST), and sea level pressure (SLP) is studied via coupled nonlinear Laplacian spectral analysis, and families of modes that capture reemergence are constructed. In model configurations with ocean-to-atmosphere coupling, these "reemergence families" display a pan-Arctic scale organization of SIC anomalies, related to SLP teleconnection patterns. The ocean is found to provide the key source of memory for reemergence, as an SST-based reemergence mechanism can operate as a stand-alone process, while an SLP-based mechanism cannot. Dynamical feedback from the ocean to the atmosphere is found to be essential in creating large-scale organized patterns of SIC-SLP covariability.

1. Introduction

Satellite observations since 1979 have documented rapid changes in Arctic sea ice, spurring increased focus on Arctic prediction and predictability [e.g., *Stroeve et al.*, 2014; *Tietsche et al.*, 2014; *Guemas et al.*, 2014]. A key element of this effort is the identification of physically based mechanisms for sea-ice predictability. Sea-ice reemergence, a phenomenon in which sea-ice area anomalies tend to recur at time lags of 5–12 months, is an example of one such mechanism, originally identified by *Blanchard-Wrigglesworth et al.* [2011]. Sea-ice reemergence is observed in two main forms: (1) a melt season to growth season reemergence (henceforth, melt-to-growth reemergence), related to the imprinting and summer persistence of sea surface temperature (SST) anomalies in the seasonal ice zones, and (2) a growth season to melt season reemergence (henceforth, growth-to-melt reemergence), related to winter persistence of sea-ice thickness (SIT) anomalies in the central Arctic [*Blanchard-Wrigglesworth et al.*, 2011; *Holland et al.*, 2013; *Day et al.*, 2014; *Bushuk et al.*, 2014, 2015]. Note that melt-to-growth and growth-to-melt reemergence have been termed spring-to-fall and summer-to-summer reemergence, respectively, in earlier works.

The study of *Bushuk et al.* [2015] also identified an atmospheric role in melt-to-growth reemergence, relating reemerging sea-ice concentration (SIC) patterns to pan-Arctic scale sea level pressure (SLP) teleconnection patterns. These patterns closely resemble the Arctic Dipole Anomaly (DA) [*Wu et al.*, 2006] and Arctic Oscillation (AO) [*Thompson and Wallace*, 1998] patterns of SLP variability. This study corroborated earlier findings on the SST-SIC melt-to-growth reemergence mechanism [*Blanchard-Wrigglesworth et al.*, 2011; *Holland et al.*, 2013; *Day et al.*, 2014; *Bushuk et al.*, 2014] and suggested a possible SLP-SIC mechanism, in which SIC anomalies reemerge due to winter-to-winter regime persistence of large-scale atmospheric circulation patterns. *Bushuk et al.* [2015] did not quantify the relative importance and possible interdependence of these two mechanisms. In particular, memory sources, such as the ocean, sea ice, or snow cover, are likely crucial elements of the winter-to-winter atmospheric regime persistence that underlies the SLP-SIC mechanism. In the present work, we explore a model hierarchy to gain insight into the relative roles of the ocean and the atmosphere in producing sea-ice reemergence. Our main finding is that the SST-SIC mechanism can exist as a stand-alone process, while the SLP-SIC mechanism cannot. Nevertheless, the atmosphere is found to play a crucial role in setting SIC patterns of reemergence, particularly in models that have ocean-to-atmosphere coupling.

Sea-ice reemergence requires two elements: (1) a source of variability to create initial sea-ice anomalies and (2) a source of memory, which allows these anomalies to reemerge at some time in the future. Reemergence has been studied in observations and comprehensive climate models, both of which involve full physics and fully coupled ocean, atmosphere, and sea-ice components. In this study, we analyze a hierarchy of climate models, designed to probe different aspects of oceanic and atmospheric variability and memory. Summarized

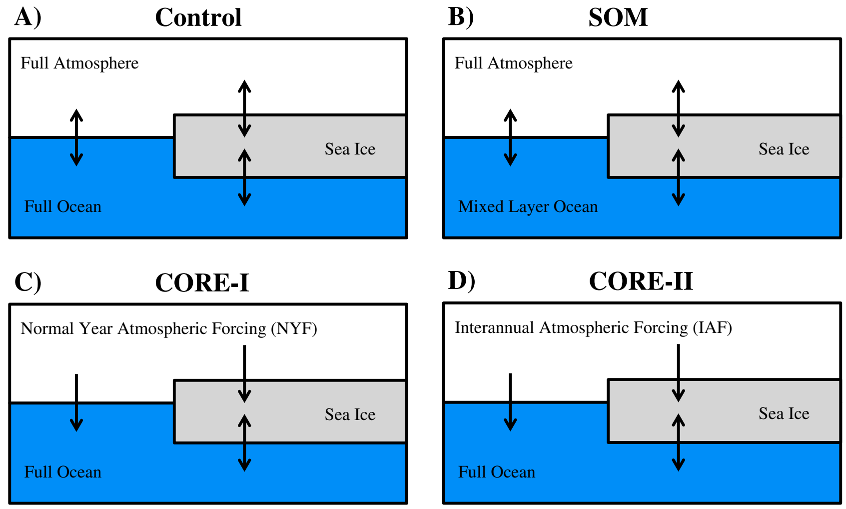

Figure 1. Schematic of the different Community Climate System Model version 4 (CCSM4) runs analyzed in this study. Arrows indicate coupling between different components of the atmosphere-ocean-sea-ice system.

in Figure 1, these models consist of a fully coupled control run, a slab ocean model (SOM) which has reduced oceanic memory and no circulation, and two coordinated ocean-ice reference experiments (COREs) which have active sea-ice-ocean components forced by normal-year and interannually varying surface fields and lack ocean-to-atmosphere coupling. Using this model hierarchy, we perform a cross-model comparison with particular focus on (1) the pan-Arctic, regional, and temporal aspects of sea-ice reemergence, (2) the relationship between sea-ice reemergence and SLP teleconnections, and (3) the representation of SST-SIC and SLP-SIC reemergence mechanisms.

2. Model Hierarchy and Methods

2.1. CCSM4 Model Hierarchy

We examine a hierarchy of global climate model (GCM) experiments from the Community Climate System Model version 4 (CCSM4) [*Gent et al.*, 2011], summarized in Figure 1. The fully coupled CCSM4 realistically simulates many aspects of Arctic climate, including the SIT distribution and SIC field [*Jahn et al.*, 2012]. CCSM4 has known Arctic SLP biases, particularly a Beaufort high which is too weak and an SLP field that is generally biased low relative to reanalysis data [*de Boer et al.*, 2012]. We use the 1300 year CCSM4 preindustrial control run, which has 1° nominal resolution in the ocean, sea-ice, and atmosphere components and is forced with 1850 greenhouse gas levels.

The SOM is the "CCSM4-NEWSOM," as described in *Bitz et al.* [2012]. The SOM has identical ice-atmosphere components to the control run, a mixed-layer ocean, and is forced with 1850 greenhouse gas levels. The mixed-layer depth (MLD), computed from the preindustrial control run, is spatially varying but fixed in time. The SOM also includes a "Q-flux" term, which accounts for changes to mixed-layer heat content due to ocean heat transport convergence. The Q-flux term, computed offline using the control run, is spatially varying and has a seasonal cycle. The SOM run is 60 years long and shares the same grid as the control run.

The CORE runs have identical ice-ocean components to the control run and are forced using surface fields from phase I (CORE-I) [*Griffies et al.*, 2009] and phase II (CORE-II) [*Danabasoglu et al.*, 2014] of the CORE forcing [*Large and Yeager*, 2004, 2009], which are based on National Centers for Environmental Prediction reanalysis as well as satellite and in situ data. The 950 year CORE-I run is forced by normal-year forcing version 2 [*Large and Yeager*, 2009], which is a repeated climatological mean annual cycle of atmospheric state variables and fluxes. The CORE-II run is forced by interannually varying forcing version 2 [*Large and Yeager*, 2009], which is an estimate of the atmospheric state over the 60 year period from 1948 to 2007. In order to focus on internal variability, we detrend the CORE-II data by subtracting monthly linear trends.

We also compare CCSM4 results to 36 years (January 1979 to December 2014) of SIC satellite observations from the Met Office Hadley Center Sea-Ice and Sea Surface Temperature (HadISST) [*Rayner et al.*, 2003] data set. We detrend the HadISST data by subtracting monthly linear trends. All data are monthly averaged, and the seasonal cycle is not removed. Retaining the seasonal cycle is crucial for our analysis of reemergence using spatiotemporal modes of variability.

2.2. Data Analysis Methods

In this work we utilize coupled nonlinear Laplacian spectral analysis (NLSA), a data analysis algorithm that extracts temporal and spatiotemporal modes of variability in multivariate data sets [*Bushuk et al.*, 2014, 2015], without requiring initial normalization of the input fields. For each model, we recover temporal and spatiotemporal modes for SIC, SST, and SLP and use these modes to investigate sea-ice reemergence. These SIC, SST, and SLP modes are inherently coupled via the multivariate NLSA kernel operator, which provides a natural comparison between variables with different physical units and is designed to emphasize states in which these fields covary strongly. The NLSA kernel is a local analog to the temporal covariance operator and is designed to extract intrinsic timescales of dynamical systems [*Giannakis and Majda*, 2012a, 2012b, 2013; *Berry et al.*, 2013], including intermittent-type modes, which are crucial for explaining reemergence. We refer the reader to *Bushuk et al.* [2015] and Text S1 in the supporting information for more details on the coupled NLSA methodology and implementation.

Coupled NLSA captures periodic modes, which represent the seasonal cycle, low-frequency modes, which capture interannual-to-decadal variability, and intermittent modes, which reflect the interaction of this periodic and low-frequency variability, in both space and time. Following *Bushuk et al.* [2015], reemergence mode families are constructed as the minimal set of SIC modes able to qualitatively reproduce the reemergence signal of the raw SIC data. For each model, we identify a five-mode reemergence family, consisting of a low-frequency mode, and degenerate pairs (same singular value) of annual and semiannual intermittent modes. Removing any mode from this family degrades the representation of the reemergence signal, whereas adding additional modes does not substantially improve the representation. We also identify associated SST and SLP modes based on correlation with the temporal patterns that make up the SIC family. We refer to this joint set of SIC, SST, and SLP modes as the "reemergence family."

3. Results

3.1. Sea-Ice Reemergence in CCSM4

We begin with a comparison of regional sea-ice reemergence characteristics in the CCSM4 model runs and HadISST observations, shown in Figure 2. We assess sea-ice reemergence by computing time-lagged pattern correlations of the raw SIC anomaly field via the methodology of *Bushuk et al.* [2014, 2015]. For each initial month (from January to December) and lag (from 0 to 23 months), in Figure 2 we report the time mean pattern correlation, taken over all (month, month+lag) pairs in the SIC time series.

Over a pan-Arctic domain (0°–360° and 45°N–90°N), we find that the control and CORE-II experiments closely match the HadISST reemergence signal. Each of these displays a clear melt-to-growth reemergence, with melt season SIC anomalies positively correlated with anomalies the following growth season, despite a loss of correlation over the intervening summer months. The growth-to-melt reemergence is quite weak in each of these experiments. Note that if one performs time-lagged total area correlations via the methodology of *Blanchard-Wrigglesworth et al.* [2011], the growth-to-melt reemergence is more prominent, yet still significantly weaker than the melt-to-growth reemergence.

Consistent with earlier CCSM3 findings [*Blanchard-Wrigglesworth et al.*, 2011], the SOM melt-to-growth reemergence signal is significantly weaker than the control run. This suggests the crucial importance of a full-depth ocean and ocean circulation in obtaining a realistic representation of melt-to-growth reemergence. Ahead, we will argue that growth-to-melt reemergence is not as severely affected in the SOM.

The CORE-I run exhibits substantial sea-ice persistence and an unrealistically strong reemergence signal, likely due to the absence of interannual variability in the atmospheric forcing fields. This suggests that internal ocean variability alone is insufficient to reduce the reemergence signal to reasonable levels. Also, the SIC variability of CORE-I dramatically underestimates that of observations. The ratio of area-integrated variance in CORE-I versus HadISST is 0.01. As a comparison, the ratios are 0.72, 0.53, and 0.56 for the control, CORE-II, and SOM runs, respectively. This indicates that a reasonable representation of atmospheric variability is essential to producing realistic sea-ice variability and reemergence.

Next, we examine the regional reemergence signals in the Bering (165°E–160°W and 55°N–65°N), Barents-Kara (30°E–90°E and 65°N–80°N), and Labrador (70°W–40°W and 45°N–80°N) Seas. The CORE-I

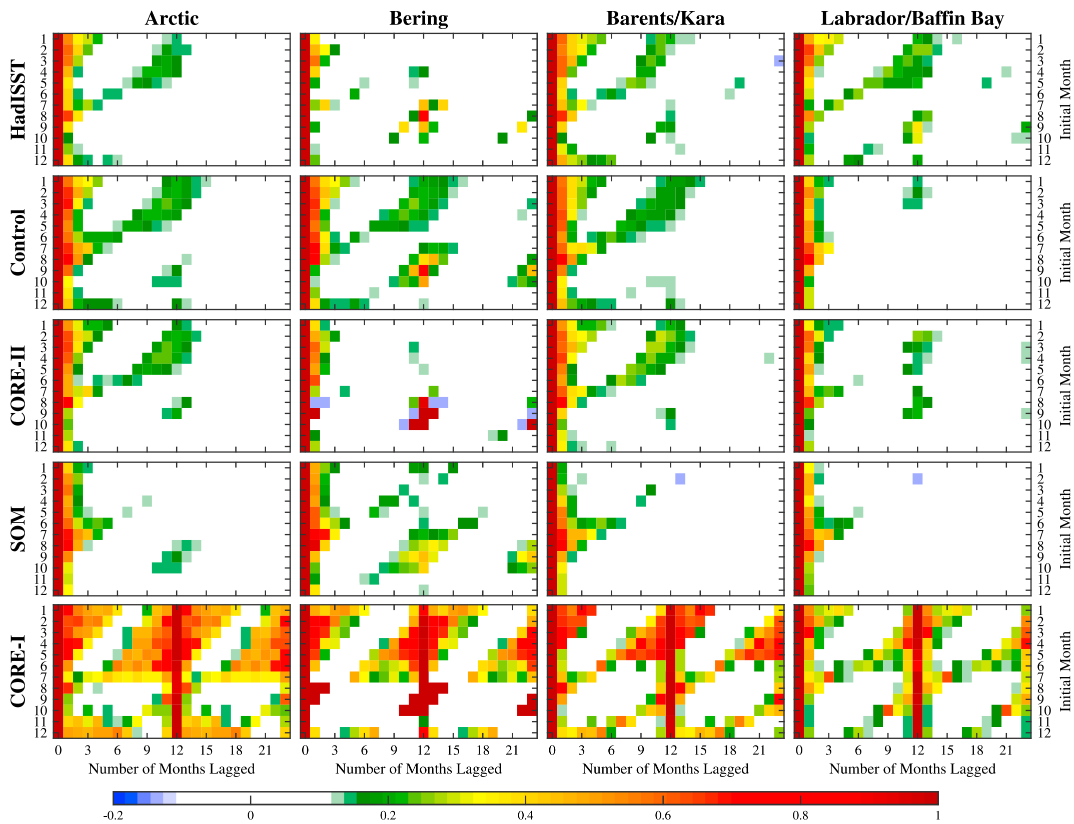

Figure 2. Time-lagged pattern correlations of SIC anomalies, computed for HadISST observations and various CCSM4 model runs, over different regions of the Arctic. All colored boxes are significant at the 95% level, based on a *t* test.

reemergence signal is too strong in all regions, relative to observations. The SOM reemergence signals are consistently weaker than the control run and are slightly enhanced in the Bering Sea.

We find that the CORE-II run is a better match with observations than the control simulation. Specifically, matching observations, CORE-II has weak reemergence signals in the Bering Sea and Sea of Okhotsk (not shown), whereas the control has strong reemergence signals in these regions. CORE-II qualitatively agrees with observations in all regions, except the Labrador Sea/Baffin Bay region, where it has a weak reemergence signal. This weak reemergence signal in Labrador Sea/Baffin Bay is a robust feature across all CCSM3 and CCSM4 runs that we have analyzed, likely related to the challenges of accurately modeling deep ocean convection in the Labrador Sea [*Danabasoglu et al.*, 2012]. Interestingly, *Blanchard-Wrigglesworth and Bitz* [2014] note that SIT is biased thin in the CORE-II run. Despite this SIT bias, the CORE-II SIC reemergence signal is very realistic.

Next, informed by the NLSA reemergence families, we investigate the temporal variability of sea-ice reemergence across these CCSM4 models. We compute time-lagged pattern correlations of the raw SIC data, both for the full time series, and conditional on times in which the low-frequency SIC mode of each reemergence family is active, defined as $\left|L_1^{\mathrm{SIC}}\right| > 2$ for the control and $\left|L_1^{\mathrm{SIC}}\right| > 1.5$ for CORE-II and the SOM (which corresponds to 5%, 7%, and 13% of the data, respectively). The thresholds are lower for the CORE-II and SOM runs because these runs are shorter than the control. In all three models, we find that the conditional correlations display enhanced melt-to-growth and growth-to-melt reemergence (see Figure 3). This indicates substantial temporal variability in the strength of reemergence events across all three models and demonstrates that low-frequency NLSA modes are effective predictors of these periods of enhanced reemergence.

In the SOM, the conditional correlations show a growth-to-melt reemergence of similar strength to the control and CORE-II models, but a significantly weaker melt-to-growth reemergence. The growth-to-melt reemergence occurs due to persistent SIT anomalies in regions of the central Arctic that are fully ice-covered during winter. Since SST anomalies do not participate in this mechanism, one would expect that the simplified ocean of the SOM would not impact its representation. Conversely, in a study on Antarctic sea-ice reemergence,

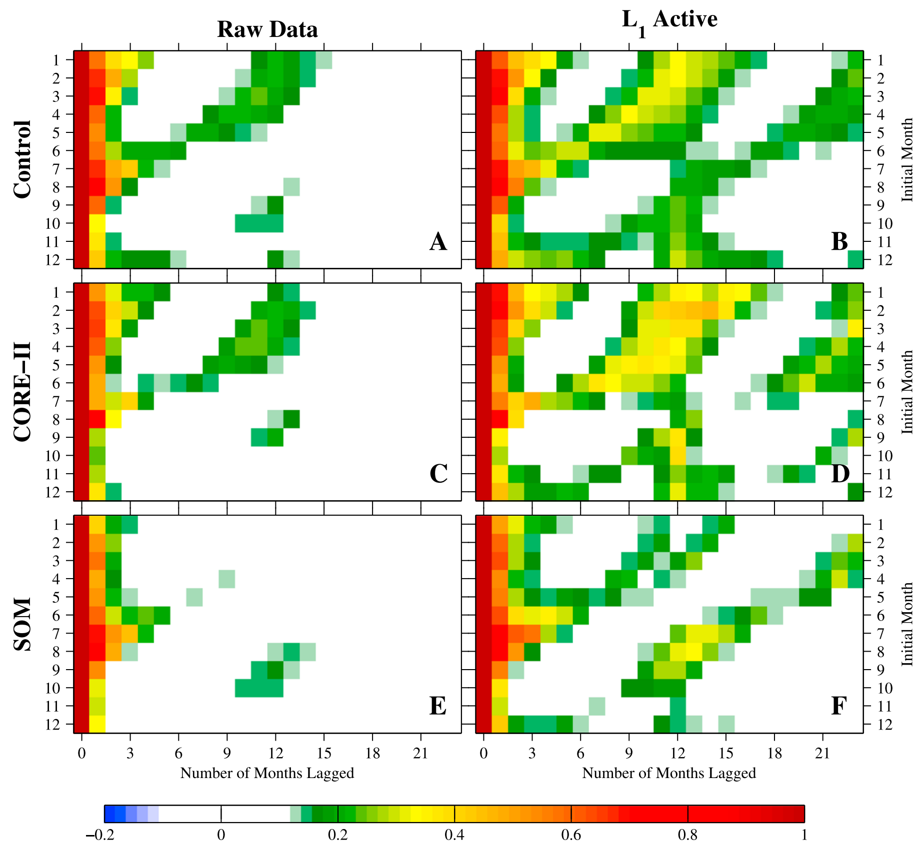

Figure 3. Time-lagged pattern correlations for different CCSM4 model runs, computed for (left column) the raw SIC anomaly data and conditional on (right column) the L_1^{SIC} mode of each reemergence family being active. All colored boxes are significant at the 95% level, based on a *t* test.

the melt-to-growth mechanism was shown to depend crucially on ocean heat storage below the mixed layer [*Holland et al.*, 2013]. Therefore, one would expect decreased fidelity of this mechanism in the SOM. The conditional lagged correlations of Figure 3 are consistent with both of these expectations.

3.2. Reemergence Mechanisms and SLP-SIC Teleconnections

We now examine the spatiotemporal evolution of the NLSA reemergence families, with particular focus on winter SIC-SLP teleconnections. Figure 4 shows winter means (January–March) of the reconstructed SIC, SST, and SLP fields of each reemergence family. These patterns are composites, computed over all times in which L_1^{SIC} of each family is active, in positive phase. Movie S1 shows the monthly evolution of these fields.

The winter SIC patterns are quite similar between the control and SOM runs, with an SIC dipole pattern between the Bering and Barents-Greenland-Iceland-Norwegian (Barents-GIN) Seas. The SIC pattern of CORE-II is dominated by anomalies in the Barents-GIN Seas and lacks the North Atlantic-North Pacific dipole that characterizes the control and SOM. It should also be noted that despite being forced by a realistic atmosphere, the CORE-II SIC pattern differs substantially from the leading observational SIC mode, whether this mode is derived via EOF analysis [*Deser et al.*, 2000] or via NLSA [*Bushuk et al.*, 2015]. The SST patterns of each family have opposite sign to the local SIC anomalies and generally reflect the melt-to-growth SST-SIC reemergence mechanism (see Movie S1). One exception to this is the Barents region of the SOM, which does not display the summer imprinting of SST anomalies seen in the northern Bering and Chukchi Seas of the SOM and in the other models. A possible reason for this is the shallow depth of the Bering Sea shelf region and Chukchi Sea (difference between model MLD and ocean depth is less than 50 m; see Figure S1), meaning the mixed-layer ocean likely provides a reasonable representation of the ocean dynamics of this region and the SST-SIC reemergence mechanism. Conversely, the Barents Sea is deeper (difference between model MLD and ocean depth is greater than 150 m) and is likely poorly represented by the SOM.

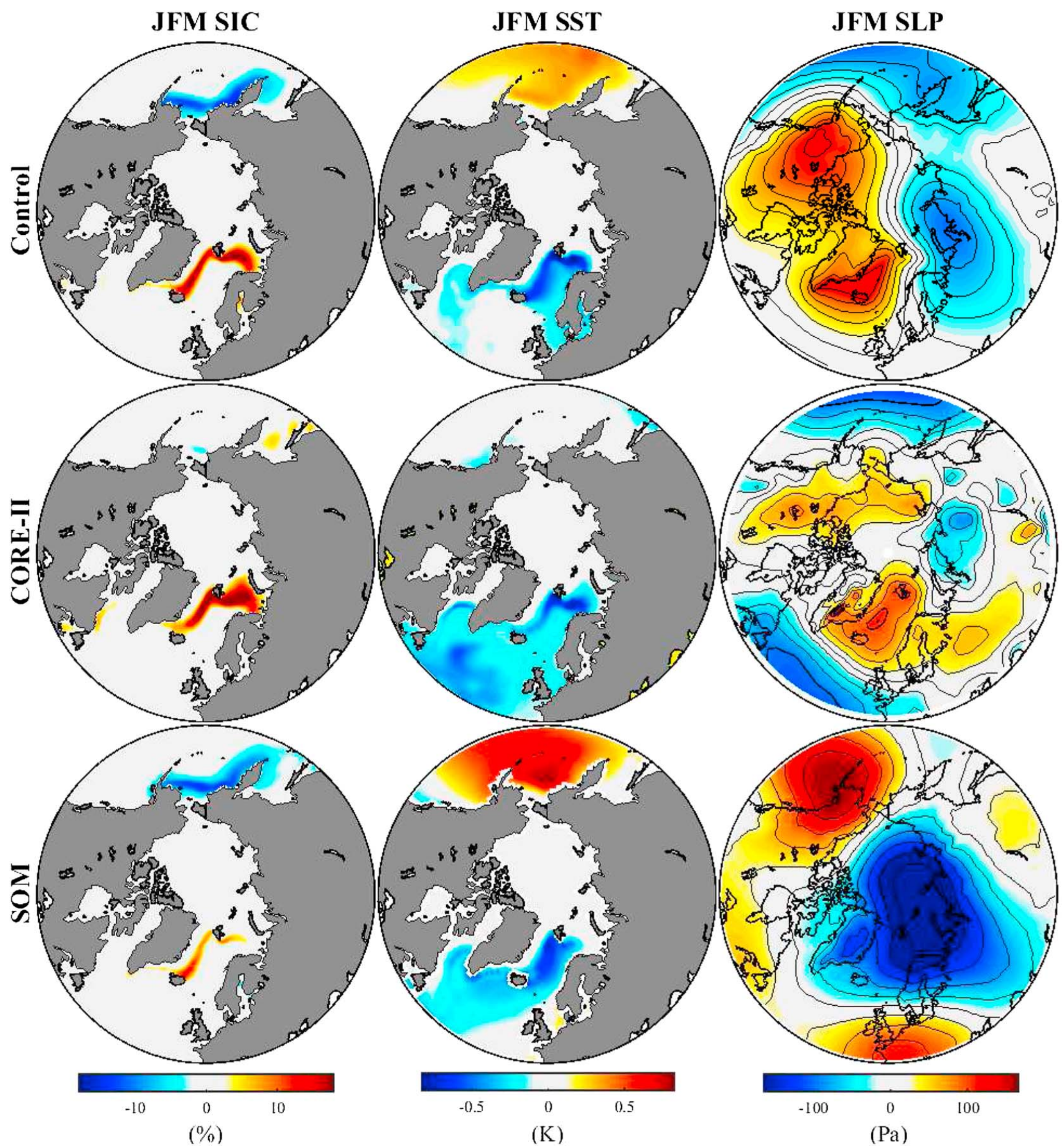

Figure 4. Boreal winter (January-February-March) composites of (left column) SIC, (middle column) SST, and (right column) SLP (SLP contours in black) are shown for reemergence families of the (top row) control, (middle row) CORE-II, and (bottom row) SOM. The composites are computed over all times in which L_1^{SIC} of each family is active, in positive phase.

The SLP patterns of each reemergence family provide a physical explanation for the intermodel differences in winter SIC. The SOM and control run have somewhat different SLP patterns but share a key common feature: an advective pathway between the North Atlantic and North Pacific basins defined via geostrophic winds. These pathways create communication between these disconnected regions, potentially providing an SLP-SIC teleconnection. In particular, the control run displays a transpolar advective pathway, and the SOM has a pathway that runs over the Canadian Archipelago. The geostrophic winds of these SLP patterns, and their associated surface-air temperature advection, tend to create SIC anomalies of opposite sign in the Bering and Barents-GIN Seas. In contrast, the CORE-II run does not exhibit an advective pathway and, correspondingly, does not display a North Atlantic-North Pacific teleconnection.

To examine this winter SLP-SIC interaction more precisely, we next consider the relationship between meridional wind and SIC in the Bering, GIN, and Barents-Kara Seas (see Figure 5). Using the reemergence families, we create indices for these regions based on spatial mean meridional winds and spatial mean SIC anomalies and normalize these indices by the maximum standard deviation over the three regions. In regions of SLP-SIC

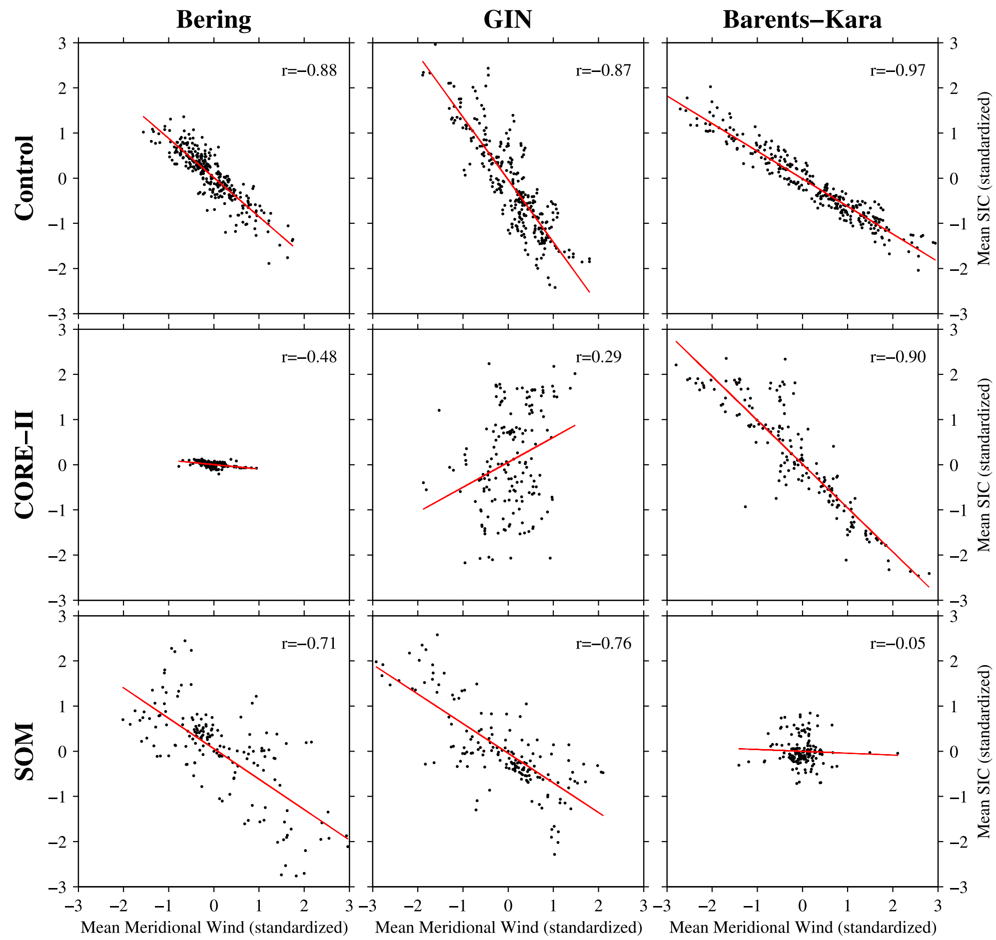

Figure 5. Scatterplots of standardized mean SIC versus mean meridional wind for the control, CORE-II, and SOM. These values are computed over winter months (January-February-March) in the Bering, GIN, and Barents-Kara Seas.

covariability, we expect negative correlation between these indices, since positive meridional winds create negative SIC anomalies, and vice versa. The control run shows this negative correlation clearly in the Bering, GIN, and Barents-Kara Seas, all regions of significant SIC variability in this model. Similarly, the SOM shows negative correlations in the Bering and GIN Seas, which dominate the winter SIC variability of this model, and no relationship in the Barents-Kara Seas, which have little winter SIC variability. CORE-II shows a clear negative relationship in the Barents-Kara Seas, a weak positive relationship in the GIN Seas, and a low-variance SIC signal in the Bering Sea. The SLP-SIC relationships in CORE-II are weaker than the other models, as they can explain the Barents-Kara anomalies, but not the GIN anomalies.

A necessary condition for an SIC-SLP teleconnection is a clear negative correlation between mean meridional wind and mean SIC in at least one region of both the North Atlantic and North Pacific. The control and SOM clearly satisfy this necessary condition, but CORE-II does not. Why is this the case? A key difference between these models is the lack of ocean-to-atmosphere coupling in CORE-II (see Figure 1). In particular, CORE-II ocean heat anomalies are unable to feedback on the atmosphere and modify its state. These results suggest that this ocean-to-atmosphere coupling is essential in creating coherent pan-Arctic scale covariability of SIC and SLP.

The control and SOM display the SLP-SIC reemergence mechanism, due to their winter-to-winter SLP regime persistence (Movie S1). This mechanism is not well represented in the CORE-II run, as the SLP patterns are transient in space and do not correlate clearly with SIC anomalies (Figure 5). Conversely, the CORE-II and control runs display the SST-SIC reemergence mechanism, whereas this mechanism is not as robustly represented in the SOM. Given CORE-II's stronger and more realistic reemergence signal compared with the SOM, this suggests that the SST-SIC mechanism can operate as a stand-alone reemergence mechanism. In contrast, the SLP-SIC mechanism cannot operate as a stand-alone process, as it crucially depends on the full-depth dynamics and persistence of the ocean. This suggests that oceanic persistence is the key source of memory for sea-ice reemergence. However, this does not preclude an atmospheric role in reemergence. Given the observed pan-Arctic scale organization of SIC anomalies in the control and SOM, the atmosphere is the most likely driver of this variability, as oceanic variability does not provide a direct method of communication between different ocean basins. In runs with ocean-to-atmosphere coupling, the atmosphere provides an important dynamical linkage, setting the spatial patterns of SIC reemergence.

4. Conclusions

We have assessed the representation of Arctic sea-ice reemergence and associated SST and SLP-based mechanisms in a hierarchy of CCSM4 models. The primary conclusions of this study are the following:

1. There is good quantitative agreement of pan-Arctic reemergence between observations, the preindustrial control simulation, and the CORE-II run. On regional scales, CORE-II matches observations better than the control.
2. Relative to observations, the reemergence signals of the SOM and CORE-I are too weak and too strong, respectively. The weak SOM reemergence signal indicates the crucial role of ocean circulation and heat storage below the mixed layer in providing memory for reemergence. The unrealistically strong reemergence in CORE-I indicates the necessity of atmospheric variability in providing a realistic representation of reemergence.
3. The control, CORE-II, and SOM all exhibit substantial temporal variability in the strength of reemergence events. Low-frequency SIC modes of the NLSA reemergence families are effective predictors of periods of enhanced reemergence activity.
4. The reemergence families of the control and SOM runs exhibit a winter SLP-SIC teleconnection between the Bering and Barents-GIN Seas. The SLP patterns of the families are physically consistent with the SIC patterns and allow communication between the North Pacific and North Atlantic sectors via their geostrophic winds. The CORE-II winter SIC pattern is dominated by anomalies in the Barents-GIN Seas and does not exhibit this teleconnection. This suggests that dynamical feedback from the ocean to the atmosphere is essential in creating large-scale organized patterns of SIC-SLP covariability.
5. The control run exhibits both the SST-SIC and the SLP-SIC reemergence mechanisms. The representation of the SST-SIC and SLP-SIC mechanism is degraded in the SOM and CORE-II runs, respectively. CORE-II has a more realistic reemergence signal than the SOM, suggesting that the SST-SIC mechanism is able to operate as a stand-alone mechanism. In models with ocean-to-atmosphere coupling, atmospheric variability plays a key role in reemergence, setting the spatial patterns of SIC reemergence.

In this study, we have attempted to gain insight into the coupled nature of sea-ice reemergence, by exploring models with the same sea-ice component, but different physics and coupling of the atmosphere and the ocean. Because of the nonlinear, coupled dynamics of the atmosphere-ocean-ice system it is challenging to properly address notions of causality in this framework. Additional work, involving idealized model experiments and analysis of other GCMs, is required to further test the conclusions presented in this study. More broadly, understanding physical mechanisms underlying sea-ice variability may lead to advances in seasonal sea-ice forecasting through the identification of initial conditions with potentially high predictability.

Acknowledgments
We thank Cecilia Bitz for assistance in running and interpreting the CCSM4 SOM experiments and for sharing data from previous SOM experiments. We thank Andy Majda for many stimulating discussions. We also thank Steve Yeager and Keith Lindsay for sharing the CCSM4 CORE-I data set. Finally, we thank Gary Strand for preparation of the CCSM4 Control and CCSM4 CORE-II data sets. The research of D. Giannakis was supported by ONR DRI grant N00014-14-1-0150 and ONR MURI grant 25-74200-F7112. M. Bushuk is supported as a doctoral student on the first grant. The CCSM4 control and CORE-II data were downloaded from the Earth System Grid website (http://www.earthsystemgrid.org). The HadISST data were downloaded from the Met Office Hadley Centre website (http://www.metoffice.gov.uk/hadobs/hadisst/). The CORE-II forcing data were downloaded from http://data1.gfdl.noaa.gov/nomads/forms/core/COREv2.html, which is maintained by the Geophysical Fluid Dynamics Laboratory (GFDL). Data for the CORE-I and SOM runs were obtained from local disk on Yellowstone, the high-performance computing cluster at the National Center for Atmospheric Research (NCAR), and is available upon request.

The Editor thanks two anonymous reviewers for their assistance in evaluating this paper.

References

Berry, T., R. Cressman, Z. Greguric-Ferencek, and T. Sauer (2013), Time-scale separation from diffusion-mapped delay coordinates, *SIAM J. Appl. Dyn. Syst.*, *12*, 618–649.

Bitz, C., K. Shell, P. Gent, D. Bailey, G. Danabasoglu, K. Armour, M. Holland, and J. Kiehl (2012), Climate sensitivity of the community climate system model, version 4, *J. Clim.*, *25*(9), 3053–3070.

Blanchard-Wrigglesworth, E., and C. M. Bitz (2014), Characteristics of Arctic sea-ice thickness variability in GCMs, *J. Clim.*, *27*(21), 8244–8258.

Blanchard-Wrigglesworth, E., K. C. Armour, C. M. Bitz, and E. DeWeaver (2011), Persistence and inherent predictability of Arctic sea ice in a GCM ensemble and observations, *J. Clim.*, *24*, 231–250.

Bushuk, M., D. Giannakis, and A. J. Majda (2014), Reemergence mechanisms for North Pacific sea ice revealed through nonlinear Laplacian spectral analysis, *J. Clim.*, *27*, 6265–6287.

Bushuk, M., D. Giannakis, and A. J. Majda (2015), Arctic sea-ice reemergence: The role of large-scale oceanic and atmospheric variability, *J. Clim.*, doi:10.1175/JCLI-D-14-00354.1, in press.

Danabasoglu, G., S. C. Bates, B. P. Briegleb, S. R. Jayne, M. Jochum, W. G. Large, S. Peacock, and S. G. Yeager (2012), The CCSM4 ocean component, *J. Clim.*, *25*(5), 1361–1389.

Danabasoglu, G., et al. (2014), North Atlantic simulations in coordinated ocean-ice reference experiments phase II (CORE-II). Part I: Mean states, *Ocean Model.*, *73*, 76–107.

Day, J., S. Tietsche, and E. Hawkins (2014), Pan-Arctic and regional sea ice predictability: Initialization month dependence, *J. Clim.*, *27*(12), 4371–4390.

de Boer, G., W. Chapman, J. E. Kay, B. Medeiros, M. D. Shupe, S. Vavrus, and J. Walsh (2012), A characterization of the present-day Arctic atmosphere in CCSM4, *J. Clim.*, *25*(8), 2676–2695.

Deser, C., J. E. Walsh, and M. S. Timlin (2000), Arctic sea ice variability in the context of recent atmospheric circulation trends, *J. Clim.*, *13*, 617–633.

Gent, P. R., et al. (2011), The Community Climate System Model version 4, *J. Clim.*, *24*(19), 4973–4991.

Giannakis, D., and A. J. Majda (2012a), Nonlinear Laplacian spectral analysis for time series with intermittency and low-frequency variability, *Proc. Natl. Acad. Sci.*, *109*, 2222–2227.

Giannakis, D., and A. J. Majda (2012b), Comparing low-frequency and intermittent variability in comprehensive climate models through nonlinear Laplacian spectral analysis, *Geophys. Res. Lett.*, *39*, L10710, doi:10.1029/2012GL051575.

Giannakis, D., and A. J. Majda (2013), Nonlinear Laplacian spectral analysis: Capturing intermittent and low-frequency spatiotemporal patterns in high-dimensional data, *Stat. Anal. Data Min.*, *6*(3), 180–194, doi:10.1002/sam.11171.

Griffies, S. M., et al. (2009), Coordinated ocean-ice reference experiments (COREs), *Ocean Model.*, *26*(1), 1–46.

Guemas, V., et al. (2014), A review on Arctic sea-ice predictability and prediction on seasonal to decadal time-scales, *Q. J. R. Meteorol. Soc.*, doi:10.1002/qj.2401.

Holland, M. M., E. Blanchard-Wrigglesworth, J. Kay, and S. Vavrus (2013), Initial-value predictability of Antarctic sea ice in the Community Climate System Model 3, *Geophys. Res. Lett.*, *40*, 2121–2124, doi:10.1002/grl.50410.

Jahn, A., et al. (2012), Late-twentieth-century simulation of Arctic sea ice and ocean properties in the CCSM4, *J. Clim.*, *25*(5), 1431–1452.

Large, W., and S. Yeager (2009), The global climatology of an interannually varying air-sea flux data set, *Clim. Dyn.*, *33*(2–3), 341–364.

Large, W. G., and S. G. Yeager (2004), Diurnal to decadal global forcing for ocean and sea-ice models: The data sets and flux climatologies, *Tech. Rep. TN-460+STR*, Natl. Cent. for Atmos. Res., Boulder, Colo.

Rayner, N. A., D. E. Parker, E. B. Horton, C. K. Folland, L. V. Alexander, D. P. Rowell, E. C. Kent, and A. Kaplan (2003), Global analyses of sea surface temperature, sea ice, and night marine air temperature since the late nineteenth century, *J. Geophys. Res.*, *108*(D14), 4407, doi:10.1029/2002JD002670.

Stroeve, J., L. C. Hamilton, C. M. Bitz, and E. Blanchard-Wrigglesworth (2014), Predicting September sea ice: Ensemble skill of the SEARCH sea ice outlook 2008–2013, *Geophys. Res. Lett.*, *41*(7), 2411–2418, doi:10.1002/2014GL059388.

Thompson, D. W. J., and J. M. Wallace (1998), The Arctic oscillation signature in the wintertime geopotential height and temperature fields, *Geophys. Res. Lett*, *25*, 1297–1300, doi:10.1029/98GL00950.

Tietsche, S., J. Day, V. Guemas, W. Hurlin, S. Keeley, D. Matei, R. Msadek, M. Collins, and E. Hawkins (2014), Seasonal to interannual Arctic sea ice predictability in current global climate models, *Geophys. Res. Lett.*, *41*, 1035–1043, doi:10.1002/2013GL058755.

Wu, B., J. Wang, and J. E. Walsh (2006), Dipole anomaly in the winter Arctic atmosphere and its association with sea ice motion, *J. Clim.*, *19*, 210–225, doi:10.1175/JCLI3619.1.